AIP | Applied Physics Letters

Nanoscale electroresistance properties of all-oxide magneto-electric tunnel junction with ultra-thin barium titanate barrier

G. Kim, D. Mazumdar, and A. Gupta

Citation: Applied Physics Letters **102**, 052908 (2013); doi: 10.1063/1.4791699
View online: http://dx.doi.org/10.1063/1.4791699
View Table of Contents: http://scitation.aip.org/content/aip/journal/apl/102/5?ver=pdfcov
Published by the AIP Publishing

Nanoscale electroresistance properties of all-oxide magneto-electric tunnel junction with ultra-thin barium titanate barrier

G. Kim,[1,2] D. Mazumdar,[2] and A. Gupta[2,a)]
[1]*Department of Electrical and Computer Engineering, The University of Alabama, Tuscaloosa, Alabama 35487-0209, USA*
[2]*Center for Materials for Information Technology, The University of Alabama, Tuscaloosa, Alabama 35487-0209, USA*

(Received 31 August 2012; accepted 28 January 2013; published online 8 February 2013)

Tunnel electroresistance properties have been investigated at the nanoscale for prototype magneto-electric tunnel junctions (METJ) consisting of ferroelectric $BaTiO_3$ and ferromagnetic $La_{0.67}Sr_{0.33}MnO_3$ heterostructures. Combining piezoresponse force and conductive atomic force microscopy, we demonstrate robust and reproducible polarization-dependent tunneling behavior with a resistance ratio between the two polarization states as high as 60 for a 3 unit cell (~1.2 nm) $BaTiO_3$ tunnel barrier. Our work demonstrates that METJs are scalable down to barrier layer thicknesses comparable to commercial spintronic devices. © *2013 American Institute of Physics*. [http://dx.doi.org/10.1063/1.4791699]

Magnetoelectric and multiferroic tunnel junctions (METJs and MFTJs) are an emerging paradigm for device applications.[1] They provide the basis for a class of solid-state memory devices, which are non-volatile and both electrically and magnetically tunable, and sometimes referred to as magnetoelectric random access memory (MERAM) devices.[2] Fundamentally, METJs and MFTJs combine both tunnel electroresistance (TER) and tunnel magnetoresistance (TMR) effects.[3] Such heterostructures consist of an ultrathin ferroelectric or multiferroic material as the active tunneling barrier sandwiched between ferromagnetic electrodes. While room-temperature TMR effect has been known for almost 20 yr, TER effect has only been recently reported, thanks largely to advances in oxide thin-film growth.[4–8] All these experiments verify the earlier theoretical prediction of the TER effect.[9–11] More recently, proof-of-concept METJ devices have been successfully demonstrated at low temperatures.[12]

In this Letter, we investigate the thin-film heterostructure prototype consisting of ultrathin ferroelectric $BaTiO_3$ (BTO) and ferromagnetic $La_{0.67}Sr_{0.33}MnO_3$ (LSMO). We have quantified nanoscale ferroelectric and transport properties of this METJ prototype by using scanning probe microscopy techniques. Through local *I-V* measurements, we demonstrate robust TER effect in ultra-thin BTO tunnel barriers of only 1.2 nm thickness, which is thinner than the calculated critical BTO film thickness (2.4 nm).[13] Combined with earlier experimental reports,[4,14] we show that METJs have the ability to scale down (i.e., retain their functionality) to a level that current spintronics devices can offer.

The BTO/LSMO heterostructures were deposited on (001)-oriented $SrTiO_3$ substrates using the pulsed laser deposition (PLD) technique. Measurements were performed using the MFP-3D (Asylum Research) scanning probe microscope (see supplementary information S1 for details).[18] We used three commercial conductive scanning probe tips: platinum-coated silicon (DPER-18), platinum-silicide (PtSi), and diamond-coated tips (CDT) for the conducting atomic force microscopy (C-AFM) measurements. The tips vary in terms of their resistivity, contact area characteristics, and degree of degradation with usage (see Table I of supplementary information).

AFM micrographs of 2 nm BTO films grown on 30 nm LSMO bottom electrode show an atomically flat surface with root-mean-square (rms) roughness of 0.2 nm. The films are essentially free of nanodroplets that are typically associated with the PLD process (see Figure S1). Robust ferro- and piezo-electric properties of the BTO films are observed on patterned polarized regions, as seen in Figs. 1(a) and 1(b). The University of Alabama logo has been used to generate the pattern. The dark brown color corresponds to the regions poled by negative bias voltage, while the light brown region reflects the positively poled areas.

Nanoscale ferroelectric properties of the BTO layer have been quantified using switching spectroscopy piezoresponse force microscopy (PFM) method,[15] as shown in Figs. 1(c) and 1(d). The ferroelectric hysteretic behavior is clearly observed in Fig. 1(c) along with a butterfly shaped loop for the phase (Fig. 1(d)). However, a complete 180° phase reversal is not observed. This is likely due to depolarization behavior, which has previously also been observed for ultrathin films that are close to the critical thickness for ferroelectricity.[16]

To systematically control the UP-DOWN polarization states (UP implying polarization vector pointing towards the tip), a 2 μm × 2 μm square area is first poled in the downward direction using a negative tip bias of −3 V (Fig. 1(e-1)) and then a 0.7 μm × 0.7 μm square region in the center is reverse-poled by a positive tip bias of +3 V (Fig. 1(e-2)). The dark and light PFM contrast of a larger 3 μm × 3 μm square area (Fig. 1(f)) shows clearly the different polarization states in the two regions. We further have rewritten a rectangular area in the top region of the polarized pattern by applying a positive bias voltage after the initial patterning process (Fig. 1(e-3)). The re-read PFM image is seen in Fig. 1(g). We also confirmed that Fig. 1(g) image is retained for at least three days. These results indicate that ultrathin 2 nm BTO films exhibit

a)Author to whom correspondence should be addressed. Electronic mail: agupta@mint.ua.edu.

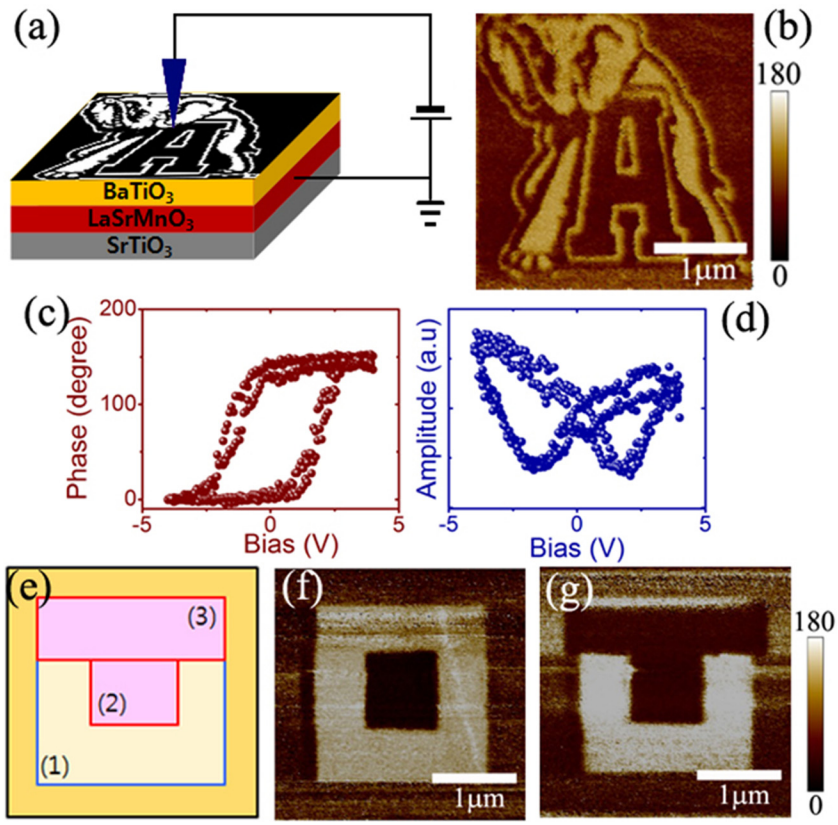

FIG. 1. (a) Schematic for generating polarization pattern. (b) Polarization image showing the UA logo with an elephant. Hysteresis loops corresponding to polarization switching of BTO film. (c) Phase map in degree and (d) amplitude map exhibiting a butterfly loop. Schematic for generating different polarization state regions. ((e)-(1)) 2 μm × 2 μm square zone poled by a negative voltage. (e-2) 1 μm × 1 μm center region poled by a positive voltage. (e-3) Re-poled area by negative voltage after 6 h. (f) PFM image after initial polarization resulting from steps (e-1) and (e-2). (g) Re-scanned PFM image after step (e-3).

robust and reproducible piezoelectric/ferroelectric properties. Qualitatively similar results have been obtained with a 1.2 nm (3 unit cells) thick BTO film on LSMO, although the PFM contrast is not as sharp as that for the 2 nm film.

Local tunneling properties of ultrathin BTO film have been investigated by measuring the current-voltage (I-V) characteristics using C-AFM technique. Measurements shown here are performed on ferroelectric BTO thin films of thickness 1.2 nm. We primarily used commercial conductive diamond-coated tips for the C-AFM measurements as they have a large tip area, which gives better contact, while the hardness of diamond provides low degree of tip wear during scans. First, we acquired current-maps where the tunnel current is measured during typical raster-scans while maintaining the tip at 1 Volt (Fig. 2). Prior to performing these measurements, an UP (DOWN) polarization state is generated by applying a high positive (negative) voltage through the sample with the tip acting as a virtual ground (Figs. 2(a) and 2(c)). In Figs. 2(b) and 2(d), we show a typical current-map of a 0.5 μm × 0.5 μm area of the BTO/LSMO heterostructure with upward and downward polarization orientations, respectively. The bright gray (green) color indicates a relatively high (low) tunnel current in the case of polarization pointing upward (downward). This is the TER effect described as the change in the resistance of the thin BTO/LSMO heterostructure arises from the switching of the polarization orientation.[9] Even though there are some local variations in the tunnel current, our data clearly show that the TER effect is robust over large areas of the BTO/LSMO heterostructure.

To further quantify the TER effect, local current (I)-voltage (V) measurements have been carried out by locally applying a sweep voltage ranging between +0.5 V to −0.5 V after creating one of the two polarization states in the sample. As Fig. 3 clearly indicates, significantly higher current (lower DC resistance) is observed for the UP state as compared to the DOWN state for all bias voltages. We refer to the high current (low resistance) state as the ON state and the low current (high resistance) state as the OFF state. Thses data, again, confirm the TER effect is robust down to a barrier thickness typically found in commercial hard-drive readheads with MgO tunnel barrier. Calculation of the resistance ratio between two polarization states reveals a value of up to

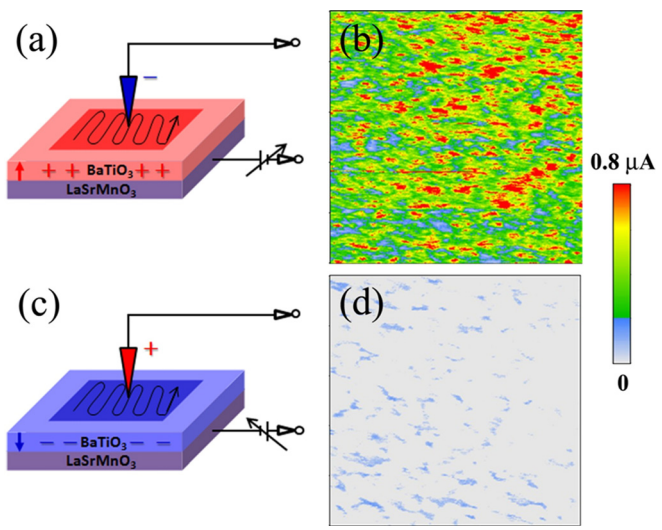

FIG. 2. Schematic of configurations for polarization orientation. (a) Polarization pointing upward by application of a positive sample bias. (b) Current map while scanning the region. (c) Polarization pointing downward by application of a negative sample bias. (d) Current map while scanning the same region. For the measurements, the tip is grounded and the current is measured using an amplifier.

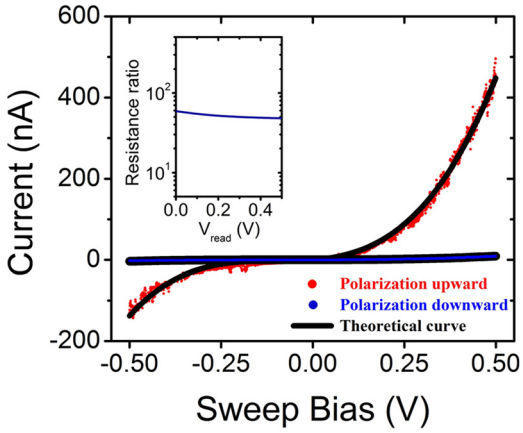

FIG. 3. I-V curves measured with different polarization states, upward or downward, corresponding to switch "ON" or "OFF" state. The black lines represent *I-V* curve fits using the Brinkman model. Insert shows the resistance ratio between two polarization states.

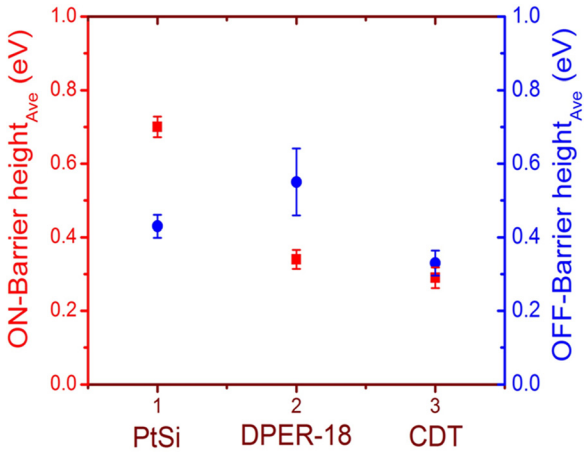

FIG. 4. Comparison of average barrier heights of polarization ON and OFF states with three different commercial tips.

60 at low bias (inset of Figure 3), which is comparable to the reported values in Ref. 5.

Detailed characterization of the TER effect has also been performed with two other commercial tips. Both PtSi and DPER-18 tips exhibit lower tunnel current (see Figures S2(a) and S2(c)), primarily because of the smaller contact area ($\sim 10^2$ nm^2). The corresponding resistance ratios between the two polarization states (Figures S2(b) and S2(d)) are also substantially smaller as compared to the conducting diamond tip, with values between 10–30 being observed at low bias voltages. We must mention that tip degradation is especially severe during local *I-V* characterization, particularly for the PtSi and DPER-18 tips, and only the few first passes with a brand new tip yield any measurable current. The characterizations shown here are, therefore, confirmed through measurements with numerous tips. Further, to account for environmental effects, we have conducted C-AFM measurement in an inert N_2 atmosphere and found that the TER effect is also robust in such conditions (see Figure S3). Taken together, while we cannot entirely eliminate the possibility of electrochemical effects influencing a part of our result, they do not appear to be determining the primary outcome of our measurements, i.e., the observation of the TER effect in ultrathin $BaTiO_3$ films.

The experimentally obtained *I-V* curves have been fitted with the Brinkman model assuming a trapezoidal potential barrier to obtain information about the average barrier height.[17] The black solid line in Fig. 3 shows the simulated *I-V* curve. As clear, the experimental points (solid red and blue dots) are well-matched with the theoretical fit (black solid lines). The fitted film thickness is between 3–4 nm, which is higher than the experimental film thickness of 1.2 nm (Table II in supplementary information). We believe that the discrepancy is due to the simplicity of the theoretical model, which does not consider experimentally involved conditions, such as interaction of the tips with the sample, BTO film surface morphology and roughness, and other tip-induced effects during the measurement.

The barrier heights determined using the different tips when fitted with the Brinkman model are compared, as shown in Fig. 4. The CDT and DPER-18 tips provide lower barrier height values for the ON state as compared to the OFF state. The average barrier height values show slight variation with the tip used, but overall in reasonable agreement with previous reports.[4,5] As expected from tunneling behavior, the average barrier height value are higher for the OFF state than the ON, except for the PtSi tip, which gives a higher barrier height value for the ON state. As Eqs. (S2)–(S5) show (see supplementary information S2 and Table II), the average barrier height and asymmetry depends only on the ratio of the fit parameters (A, B, C), which takes away any dependence on the current value. In other words, the barrier height from the Brinkman model is related to the shape of the *I-V* curve.

In conclusion, we have demonstrated robust tunnel electroresistance effect in BTO/LSMO heterostructures using piezoresponse force and conducting atomic force microscopy. Nanoscale PFM measurements clearly reveal reproducible piezoelectric properties. C-AFM characterizations are performed through current maps and current-voltage (*I-V*) curves. We demonstrate polarization-dependent and switchable tunneling current, thereby confirming the TER effect in 1.2 nm BTO film. A variety of commercial tips reveals a resistance ratio between the two polarization states between 10–60. Encouraging for commercial purposes is the result that METJs with BTO barrier can be scaled down to a thickness, which is comparable to current spintronics technology.

The work has been supported by NSF Grant No. 1102263. The MFP-3D (Asylum) used for the PFM and C-AFM characterization was acquired through DURIP (ONR) Grant No. N00014-11-1-0794.

[1]M. Ye Zhuravlev, S. S. Jaswal, and E. Y. Tsymbal, Appl. Phys. Lett. **87**, 222114 (2005).
[2]M. Bibes and A. Barthélémy, Nature Mater. **7**, 425 (2008).
[3]M. Julliére, Phys. Lett. A **54**, 225 (1975).
[4]A. Gruverman, D. Wu, H. Lu, Y. Wang, H. W. Jang, C. M. Folkman, M. Ye. Zhuravlev, D. Felker, M. Rzchowski, C.-B. Eom, and E. Y. Tsymbal, Nano Lett. **9**, 3539 (2009).
[5]A. Chanthbouala, A. Crassous, V. Garcia1, K. Bouzehouane, S. Fusil, X. Moya, J. Allibe, B. Dlubak, J. Grollier, S. Xavier, C. Deranlot, A. Moshar, R. Proksch, N. D. Mathur, M. Bibes, and A. Barthélémy, Nat. Nanotechnol. **7**, 101 (2012).
[6]H. Béa, M. Gajek, M. Bibes, and A. Barthélémy, J. Phys.: Condens. Matter. **20**, 434221 (2008).
[7]A. Crassous, V. Garcia, K. Bouzehouane, S. Fusil, A. H. G. Vlooswijk, G. Rispens, B. Noheda, M. Bibes, and A. Barthélémy, Appl. Phys. Lett. **96**, 042901 (2010).

[8]P. Maksymovych, S. Jesse, P. Yu, R. Ramesh, A. P. Baddorf, and S. V. Kalinin, Science **324**, 1421 (2009).
[9]M. Ye Zhuravlev, R. F. Sabirianov, S. S. Jaswal, and E. Y. Tsymbal, Phys. Rev. Lett. **94**, 246802 (2005).
[10]E. Y. Tsymbal and H. Kohlstedt, Science **313**, 181 (2006).
[11]H. Kohlstedt, N. A. Pertsev, J. Rodríguez, and R. Waser, Phys. Rev. B **72**, 125341 (2005).
[12]V. Garcia, M. Bibes, L. Bocher, S. Valencia, F. Kronast, A. Crassous, X. Moya, S. Enouz-Vedrenne, A. Gloter, D. Imhoff, C. Deranlot, N. D. Mathur, S. Fusil, K. Bouzehouane, and A. Barthélémy, Science **327**, 1106 (2010).
[13]J. Junquera and P. Ghosez, Nature **422**, 506 (2003).
[14]V. Garcia, S. Fusil, K. Bouzehouane, S. Enouz-Vedrenne, N. D. Mathur, A. Barthélémy, and M. Bibes, Nature **460**, 81 (2009).
[15]S. Jesse, H. N. Lee, and S. V. Kalinin, Rev. Sci. Instrum. **77**, 073702 (2006).
[16]N. A. Spaldin, Science **304**, 1606 (2004).
[17]W. F. Brinkman, R. C. Dynes, and J. M. Rowell, J. Appl. Phys. **41**, 1915 (1970).
[18]See supplementary material at http://dx.doi.org/10.1063/1.4791699 for details on growth, experimental techniques, data analysis, and additional data.